Acceleration of a plasma flow in a magnetic Laval nozzle applied to an MPD thruster

IEPC-2015-168／ISTS-2015-b-168

Presented at Joint Conference of 30th International Symposium on Space Technology and Science
34th International Electric Propulsion Conference and 6th Nano-satellite Symposium,
Hyogo-Kobe, Japan
July 4 – 10, 2015

Yohei Kobayashi [1], Kiyotaka Suzuki, Hiroaki Nabuchi, Atsushi Komuro [2], Kazunori Takahashi [3], and Akira Ando [4]

Department of Electrical Engineering, Graduate school of Engineering, Tohoku University,
6-6-05, Aoba-yama, Sendai,980-8759, Japan

Abstract: In order to clarify the acceleration mechanism of a plasma flow generated by an MPD thruster in a magnetic Laval nozzle, the electromagnetic force acting in the plasma is evaluated and plasma parameters are measured. It was found that the radial component of the electromagnetic force, F_r, is dominant in the exhaust plasma plume and the ion temperature increased at the upstream of the magnetic Laval nozzle. Additionally, measured ion Mach number increased with strength of the magnetic Laval nozzle, and this result shows good agreement with the isentropic flow model.

Nomenclature

B_0	=	uniform magnetic field strength
B_z	=	axial magnetic field strength
B_{zc}	=	magnetic diverging field strength
B_{zL}	=	magnetic Laval nozzle strength
F_r	=	radial component of the electromagnetic force
F_z	=	axial component of the electromagnetic force
T	=	particle temperature
I_d	=	discharge current
k_B	=	Boltzmann constant
M_i	=	ion Mach number
U	=	axial plasma flow velocity
γ	=	specific heat ratio

I. Introduction

Magnetoplasmadynamic thruster (MPDT) is the high power electric propulsion thruster, and the plasma is mainly accelerated by Lorentz force between the discharge current and the self-induced magnetic field. An MPDT is one of the promising candidates of main thruster in long-term and long-distance missions, such as manned interplanetary probe missions, because of it can generate the thrust significantly larger than that imparted from the

[1] Graduate student, Department of Electrical Engineering, kobayashi.yohei@ecei.tohoku.ac.jp
[2] Assistant professor, Department of Electrical Engineering, komuro@ecei.tohoku.ac.jp
[3] Associate professor, Department of Electrical Engineering, kazunori@ecei.tohoku.ac.jp
[4] Professor, Department of Electrical Engineering, akira@ecei.tohoku.ac.jp

other thrusters[1, 2]. However, there are some issues that the thrust efficiency is lower and the operation life time is shorter than other thrusters. It is reported that applying an external magnetic field to MPDT can improve the thrust performance and lower the electrode erosion[3]. Additionally, if the configuration of the applied magnetic field is diverging, additional acceleration forces, Hall acceleration and Swirl acceleration, are generated by the interaction between the applied magnetic field and the discharge current[4]. As a result, the thrust performance is improved[5-7]. In this way, external magnetic field applied to an MPDT is a key technology for its thrust performance.

In our previous research, we observed that the axial flow velocity decreases while the ion temperature increases in the magnetic divergence field. This implies that the flow energy is converted to the thermal energy in the diverging magnetic field[8]. To reduce the conversion ratio from the flow energy to the thermal energy, we adopted the magnetic Laval nozzle configuration. The effects of the magnetic Laval nozzle have been reported in our previous reports[9-11], however, the acceleration mechanism of the plasma flow in the magnetic Laval nozzle has not been fully understood yet.

In this paper, in order to clarify the detailed acceleration mechanism of the plasma flow in the magnetic Laval nozzle, plasma-induced magnetic field is measured and the electromagnetic force is estimated. And, ion temperature, plasma flow velocity, and the Mach number are estimated at various magnetic Laval nozzle configurations. Finally, we compared the experimental results with the calculated results from an isentropic flow model.

II. Experimental Apparatus

Figure 2 shows the schematic of the HITOP (HIgh density TOhoku Plasma) device of Tohoku University, and all experiments are performed in the HITOP device. It consists of a cylindrical vacuum chamber (diameter D = 0.8 m, length L = 3.3 m), an MPDT, and magnetic coils surrounding the chamber. These magnetic coils can generate a uniform filed up to 0.1 T by controlling coil current. An MPDT is installed at one end-port of the HITOP device and has a coaxial structure with a central cathode rod (10 mm outer diameter) and an annular anode (30 mm inner diameter), and operated with a Helium gas whose mass flow rate is 38 mg/sec. A discharge current of I_d=7.0 kA is supplied by a pulse-forming network system with the quasi-steady duration time of 1msec. Two solenoid coils (diverging magnetic coil and Laval nozzle coil) are set near the thruster exit to superimpose various strength of a magnetic diverging field and the magnetic Laval nozzle. The magnetic field strength is given by the sum of the uniform field B_0, the diverging magnetic field B_{zc}, and the magnetic Laval nozzle B_{zL}. Figure 3 shows the magnetic Laval nozzle configurations applied to an MPDT.

Plasma-induced magnetic fields in the plasma flow are directly measured by movable three-axial magnetic probe.

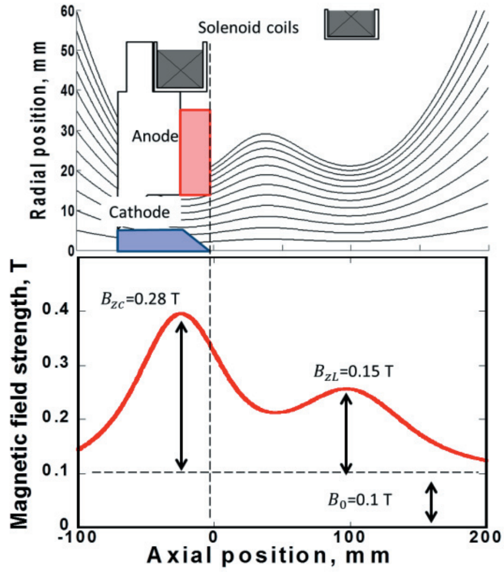

Figure 1. Magnetic field line and the strength of magnetic Laval nozzle

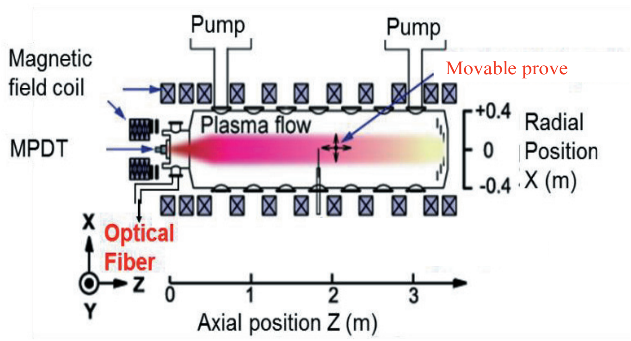

Figure 2. Schematic of the HITOP device

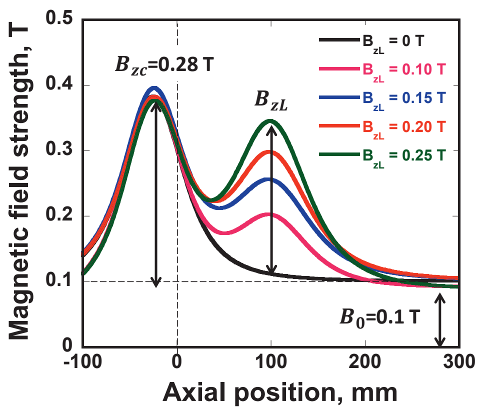

Figure 3. Magnetic field configurations

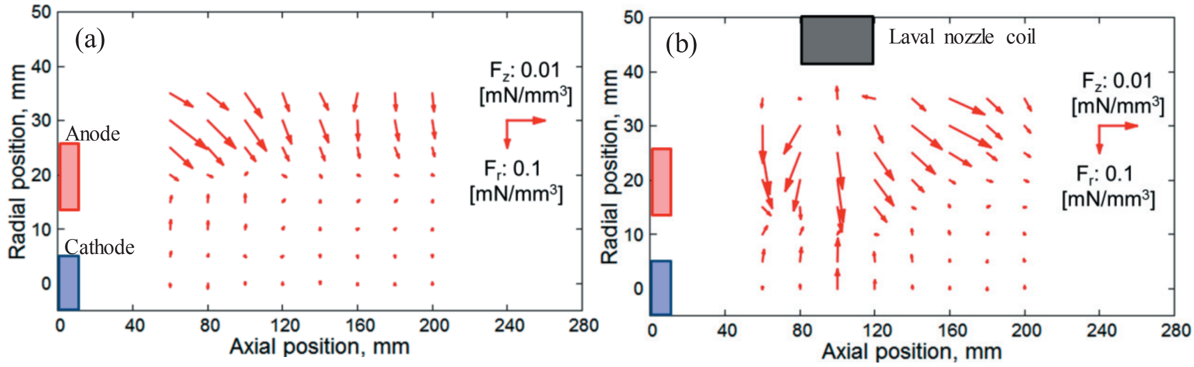

Figure 4. Two dimensional vector plots of the electromagnetic force field, (a) B_{zL}=0 T, (b) B_{zL}=0.15 T

This probe can measure the three components of the plasma – induced magnetic field ΔB_z, ΔB_r and ΔB_θ. The plasma-induced current density and the electromagnetic forces are estimated by the plasma-induced magnetic field distributions[11, 12].

Line spectrum emissions are observed to evaluate the ion velocity and ion temperature. An optical lens and a fiber are mounted on the movable stages. The light emission from the plasma is focused and passed to a Czerny–Turner spectrometer.

III. Experimental Results

A. Evaluation of Electromagnetic force field

We measured the three components of the plasma induced magnetic field by a three axial magnetic probe and estimated the spatial distribution of electromagnetic force field in the plasma flow. Plasma induced current density is calculated by Ampere's law under the assumption of the axial symmetry. Figure 4(a) and (b) show two-dimensional vector plots of axial-radial component of electromagnetic force fields F_z and F_r at B_{zL}=0 T (Only magnetic diverging field) and B_{zL}=0.15 T, respectively. In the measured region, the inward radial component of the electromagnetic force F_r is much larger than the axial component F_z. On the other hand, the integration values of the F_z in the measurement region do not change so much under the diverging magnetic field and the Laval magnetic field. These results imply that the plasma pressure increases at the upstream region of the nozzle under the Laval magnetic field.

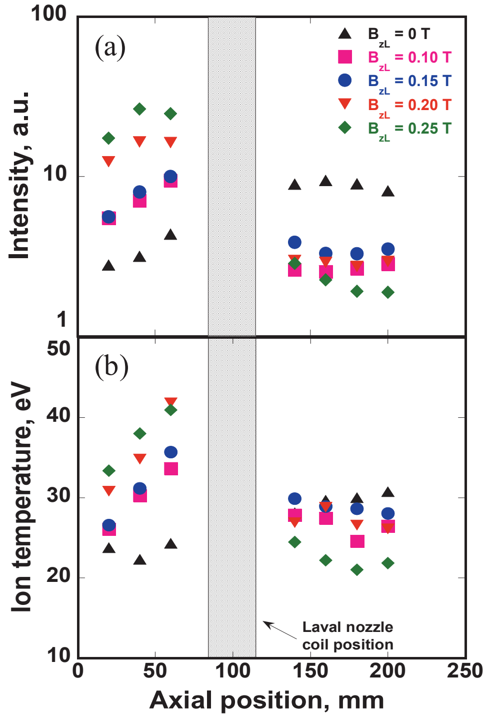

Figure 5. Axial profile of (a) emission intensity and (b) ion temperature at magnetic Laval nozzle strength B_{zL}=0 T (triangles), 0.10 T (squares), 0.15 T (circles), 0.20 T (down triangles) and 0.25 T (diamonds)

B. Emission intensity and Ion temperature

We estimated the ion temperature using an optical emission spectroscopy. Wavelength of the measured spectrum is He II line, 468.575 nm[13, 14]. The ion temperature T_i is obtained from the line broadening of the He II lines $\Delta\lambda_{1/e}$,

$$T_i = m_i (c\Delta\lambda_{1/e} / \lambda_0)^2 / 2k_B \tag{1}$$

, where m_i is particle mass, k_B is Boltzmann constant, $\lambda_{1/e}$ is 1/e half width of the measured spectrum. Axial profiles of the emission intensity and ion temperature are shown in figure 5(a) and (b), respectively. Shaded region shows the location of the Laval nozzle coil corresponding to the magnetic nozzle throat set at 10 cm downstream of the MPD thruster. In these result, both of the emission intensity and ion temperature increased at the upstream and decreased at the downstream of the magnetic Laval nozzle compared to B_{zL}=0 T. These results indicate that the

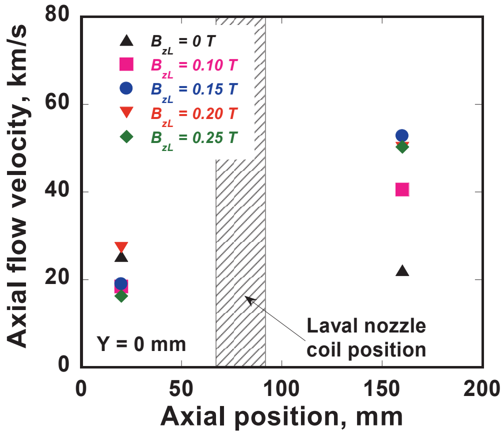

Figure 6. Axial profile of axial flow velocity at various magnetic Laval nozzle strength.

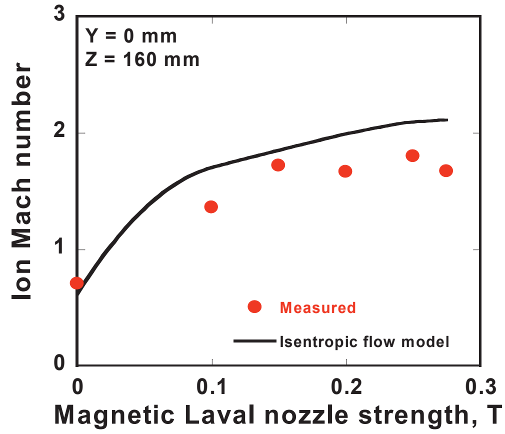

Figure 7. Dependence of the measured Mach number (circles) and caluculated Mach number from the isentropic flow model (solid line) at the magnetic Laval nozzle strength at Z=160 mm.

plasma pressure, which is estimated from the ideal gas law, increased at the upstream region of the magnetic Laval nozzle.

C. Axial flow velocity and Ion Mach number

We investigated the contribution of the magnetic Laval nozzle strengths on the axial plasma flow velocity. Axial flow velocity U is estimated using the Doppler shift $\Delta\lambda_D$,

$$U = c(\Delta\lambda_D / \lambda_0 \sin\varphi) \tag{2}$$

, where c is the light speed, λ_0 is the wavelength of the measured spectrum,468.575 nm, λ_D is the axial component of the Doppler shift, and φ is the angle between the perpendicular and oblique lines (φ=20°). Figure 6 shows a axial profile of the axial flow velocity applying the several magnetic Laval nozzle strength. The flow velocity increases with the magnetic Laval nozzle strength. However, the flow velocity is saturated when the magnetic Laval nozzle strength increases more than 0.15 T. In order to explain the increase in the flow velocity by the magnetic Laval nozzle strength and the subsequent saturation, we compared the present results with the calculated results which are obtained from the isentropic flow model. Ion Mach number M_i is defined by ratio of flow velocity U to an ion acoustic velocity Cs,

$$M_i = U / C_s = U / \sqrt{k_B(\gamma_e T_e + \gamma_i T_i) / m_i} \tag{3}$$

, where T_e and T_i are electron and ion temperatures, and γ_e and γ_i are the specific heat ratios for electrons and ions, respectively. It is well-known that when the solid nozzle cross sectional area gradually changes, the Mach number changes according to the isentropic flow model[15, 16], which is based on the aerodynamics,

$$dM / M = [2 + (\gamma_i - 1)M^2 / 2(M^2 - 1)](dA / A) \tag{4}$$

, where A is the cross section. We assumed that the magnetic flux B_zA is constant to estimate the cross section A and M_i is unity at Z=100 mm, the throat of the magnetic Laval nozzle, specific heat ratio γ_e=1.0 and γ_i=5/3. Dependence of measured Mach number and isentropic flow model at Z=160 mm on the magnetic Laval nozzle strength are shown in figure 7. It is found that the plasma flow is accelerated up to supersonic flow applying a magnetic Laval nozzle, and measured Mach number is in good agreement with the calculated Mach number using by the isentropic flow model. It indicates that acceleration mechanism of the plasma flow in the magnetic Laval nozzle is similar to the neutral gas flow in the solid Laval nozzle, that is, the plasma flow is accelerated aerodynamically in the magnetic Laval nozzle.

IV. Conclusion

We evaluated the electromagnetic force field and measured the plasma parameters in the magnetic Laval nozzle in order to understand the detailed acceleration mechanism of a plasma flow produced by an MPDT. It was found that the radial component of electromagnetic force is dominant resulting in an increase of the plasma pressure at the upstream region of the magnetic Laval nozzle. From the optical emission spectroscopy, it was found that the ion temperature increased upstream of the magnetic Laval nozzle, suggesting the increase of the plasma pressure. Mach number estimated from the measured axial flow velocity and ion temperature has qualitatively good agreement with the calculated results which are obtained from the isentropic flow model. It is revealed that aerodynamic acceleration is occurred in the magnetic Laval nozzle as well as the solid one.

References

[1]Jahn, R. G., *Physics of Electric Propulsion*, McGraw-Hill, New York, 1968.

[2]Choueiri, E. Y., and Ziemer, J. K., "Quasi-Steady Magnetoplasmadynamic Thruster Performance Database", *Journal of Propulsion and Power*, Vol. 17, No. 5, 2001, pp. 967-976.

[3]Tahara, H., Kagaya,Y., and Yoshikawa,T., "Performance and Acceleration Process of Quasisteady Magnetoplasmadynamic Arcjets with Applied Magnetic Fields", *Journal of Propulsion and Power*, Vol. 13, No. 5, 1997, pp. 651-658.

[4]Sasoh, A., "Simple formulation of magnetoplasmadynamic acceleration", *Physics of Plasmas*, Vol. 1, No. 3, 1994, pp. 464-469.

[5]Coletti, M., "A thrust formula for an MPD thruster with applied-magnetic field", *Acta Astronautica*, Vol. 81, 2012, pp. 667-674

[6]Albertoni, R., Paganucci, F., Rossetti, P., and Andrenucci, M., "Experimental Study of a Hundred-Kilowatt-Class Applied-Field Magnetoplasmadynamic Thruster", *Journal of Propulsion and Power*, Vol. 29, No. 5, 2013, pp. 1138-1145.

[7]Boxberger, A., Bambach, P., Herdrich, G., Fasoulas, S., Roser, H., P., Merio, M., and Ahedo, E., "Experimental Investigation of Steady State AppliedField Magnetoplasmadynamic Thrusters at Institute of Space System", AIAA-Paper 2012-4012, 2012

[8]Izawa, Y., Suzuki, K., Takahashi, K., and Ando, A., "Effect of a Magnetic nozzle in an MPD thruster", *Proceedings of the 12th Asia Pacific Physics Conference*, Vol. 1, 015046, 2014.

[9]Inutake, M., Ando, A., Hattori, K., Tobari, H., Makita, T., Shibata, M., Kasashima, Y., and Komagome, T., "Generation of supersonic plasma flows using an applied-field MPD arcjet and ICRF heating", *Plasma Physics and Controlled Fusion*, Vol. 49, No. 5A, pp. A121-A134.

[10]Inutake, M., Ando, Hattori, K., Tobari, H., Harata, K., and Komagome, T., "Improvement of an MPD Thruster Performance with a Laval-type Magnetic Nozzle", *Proceedings of the 29th International Electric Propulsion Conference*, IEPC-2005-83, 2005.

[11]Tobari, H., Inutake, M., Ando, A., and Hattori, K., "Spatial Distribution of Lorentz Forces in an Applied-Field Magneto-Plasma-Dynamic Arcjet Plasma", *Journal of Plasma and Fusion Research*, Vol. 80, No. 8, 2004, pp. 651-652.

[12]Tobari, H., Inutake, M., Ando, A., and Hattori, K., "Characteristics of electromagnetically accelerated plasma flow in an externally applied magnetic field", *Physics of Plasmas*, Vol. 14, No. 9, 2007.

[13]Ando, A., Ashino, M., Sagi, Y., Inutake, M., Hattori, K., Yosinuma, M., Imasaki, A., Tobari, H., and Yagai, T., "Spectroscopic Studies of a High Mach-Number Rotating Plasma Flow", *Journal of Plasma Physics and Controlled Fusion SERIES*, Vol. 4, 2001, pp. 373-378.

[14]Inutake, M., Ando, A., Hattori, K., Tobari, H., Makita, T., and Isobe, H, "Transonic Plasma Flow Passing Through a Magnetic Mirror", *Transactions of Fusion Science and Technology*, Vol. 51, No. 2T, 2007, pp. 141-146.

[15]Inutake, M., "Elements of Flow and Shock in Conventional Gasdynamics", *Journal of Plasma and Fusion Research*, Vol. 83, No. 1, pp. 62-65.

[16]Streeter, V. L., *Fluid mechanics*, McGraw-Hill, New York, 1971, pp. 335-341.